Civil Engineering Beyond Limits 1 (2027) 11179
Civil Engineering Beyond Limits
journal home: www.acapublishing.com/journals/1/cebel

Research Article

Precursor-Dependent Performance of Low-Silicate-Modulus Industrial Byproduct-Based Geopolymers

Hüseyin Ersoy[1], Murat Çavuş[*,2], İlhami Demir[1]
[1]Department of Civil Engineering, Kırıkkale University, 71460 Kırıkkale, Türkiye
[2]Department of Civil Engineering, Tokat Gaziosmanpasa University, 60150 Tokat, Türkiye

Keywords

Fly ash,
Geopolymer,
Loss on ignition,
Silicate modulus,
Mechanical performance,
Granulated blast furnace slag.

Abstract

This study examined 16 alkaline-activated paste formulations using granulated blast-furnace slag (GBFS) and fly ash from Çatalağzı (CAT), Kemerköy (KEM), and Kangal (KAN). Four nominal silicate moduli (0.2, 0.4, 0.6, and 0.8) were tested, with the water content of each precursor being adjusted using a Vicat-based consistency criterion. All specimens were heat-treated at 60 °C for 24 hours. The density, ultrasonic pulse velocity, and mechanical performance of the specimens were assessed in relation to the composition, fineness, and morphology of the precursors. The water-to-binder ratios ranged from 0.251–0.259 for CAT to 0.688–0.699 for KAN. GBFS achieved peak compressive and flexural strengths of 82.25 and 4.91 MPa, respectively, at a nominal modulus of 0.6 with a maximum ultrasonic pulse velocity of 3.65 km/s. CAT performed best at a modulus of 0.6, while KEM achieved its highest mechanical performance at a modulus of 0.4. KAN exhibited a loss-on-ignition of 9.60%, high water demand, bleeding, declining density, and low strength. Its density decreased by 8.45% between days 1 and 28, but this does not directly correlate with porosity. Differences in water content complicate strength comparisons across precursors, while changes in alkaline dosage limit the interpretation of modulus effects. Therefore, the best-performing formulations depend on the consistency and curing conditions used. These results highlight the importance of considering activator composition, precursor properties, and water demand together.

1. Introduction

While Ordinary Portland Cement (OPC) remains the predominant binder in the construction industry, its production is increasingly scrutinized due to substantial energy consumption and adverse environmental impacts [1, 2]. In the cement production process, raw materials are heated at high temperatures, a procedure that requires a significant amount of energy [3]. It has been reported that this high energy consumption, combined with the carbon dioxide released from $CaCO_3$ at temperatures above 900 °C, accounts for approximately 7% of global CO_2 emissions [4]. Due to this negative impact on climate change, researchers and industry representatives are increasingly exploring alternative binders [6]. In recent years, geopolymers and alkali-activated materials, which often utilize industrial waste, have garnered considerable interest as potential alternatives to Portland cement [7, 8].

Geopolymers are inorganic binders formed through the alkaline activation of aluminosilicate-rich precursors [9,10]. Natural materials such as metakaolin and industrial by-products, including silica fume, fly ash, and granulated blast furnace slag (GBFS), can be used in these binder systems [11–13]. Their appeal lies in the opportunity to reuse industrial by-products, potentially reduce carbon emissions, and achieve good mechanical performance under suitable production conditions [14]. However, the reaction products and resulting microstructure vary with the chemical and physical characteristics of the precursor [15].

Sodium hydroxide (NaOH), potassium hydroxide (KOH), sodium silicate (Na_2SiO_3) and potassium silicate (K_2SiO_3) are commonly used activators [16, 17]. A key consideration in mixture design is the silicate modulus (Ms), which expresses the ratio of soluble silica to alkali in the activator. Changes in Ms influence the dissolution of the precursors, the formation of the reaction products and the development of the strength [18, 19, 15]. At higher moduli, increased dissolved silica can hinder dissolution of the precursors, whereas lower moduli generally provide a more alkaline environment, altering the reaction process and microstructure [20, 21]. The most favorable Ms therefore depends on the precursor and the other mixture parameters.

Loss on ignition (LOI), specific surface area and chemical composition also influence alkali activation. In fly ash, LOI is commonly used as an indirect indicator of unburned carbon, although it does not measure carbon content alone [22]. A high LOI reading may be associated with a greater demand for water and reduced workability, which can potentially increase porosity when additional mixing water is required [23]. A larger specific surface area can promote dissolution by increasing the contact area between the precursor and the activating solution [24, 25]. The relative amounts of SiO_2, Al_2O_3 and CaO also govern the nature and development of reaction products [26, 27]. Accordingly, low-calcium Class F and high-calcium Class C fly ashes can respond differently to alkaline activation [28].

This study examines four industrial by-products: slag from İskenderun and fly ash from Çatalağzı, Kemerköy, and Kangal. These sources exhibit varying levels of calcium, LOI values, fineness, and particle morphology within a single experimental program. Their use is relevant to the valorization of residues from iron production and coal combustion. However, the study did not quantify plant-specific production volumes,

*Corresponding Author: murat.cavus@gop.edu.tr
Received 05 Sep 2026; Revised 19 Oct 2026; Accepted 26 Oct 2026
https://doi.org/10.36937/cebel.2027.11179
2687-5756 /© 2022 The Authors, Published by ACA Publishing; a trademark of ACADEMY Ltd. All rights reserved.

disposal practices, or transport costs. The low nominal modulus range of 0.2–0.8 tests whether useful performance can be obtained with a relatively low soluble-silica-to-alkali ratio. Potential savings in silicate use or processing costs require a separate assessment, since hydroxide demand and heat curing can offset such benefits. The objective is to compare consistency-adjusted formulations and identify the modulus that performs best in terms of consistency, rather than isolating an intrinsic chemical optimum at constant water content. Water demand, density, ultrasonic pulse velocity, and strength are considered alongside the measured precursor properties.

2. Materials and Testing Process

2.1. Test specimens and properties

Granulated blast furnace slag (GBFS) was obtained from the İskenderun Iron and Steel Factory. Fly ashes were sourced from the Çatalağzı (CAT), Kemerköy (KEM) and Kangal (KAN) thermal power plants. CAT is described as Class F and KEM and KAN as Class C in the source characterization, with reference to ASTM C618 [26]. These labels do not establish compliance with every requirement of that specification. Table 1 presents XRF oxide compositions, LOI, density and Blaine specific surface area. Particle size distributions and precursor SEM images are shown in Figures 1 and 2. These images characterize the unreacted feedstocks, not the hardened reaction products. Quantitative XRD phase fractions are not available in the present dataset. Thus, reactive glass content cannot be calculated from the XRF totals, and the discussion does not equate total CaO or aluminosilicate content with reacted fractions [14].

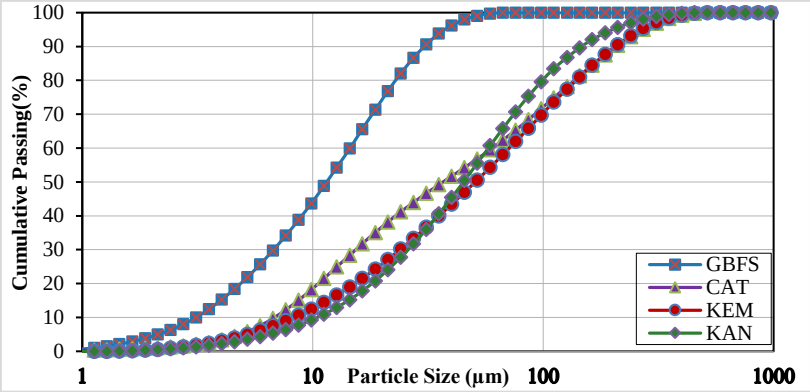


Figure 1. Particle size distribution of binder materials

Table 1. Chemical composition and physical properties of the binder materials

Binder	SiO2	Al2O3	Fe2O3	CaO	MgO	K2O	TiO2	SO3	Na2O	LOI*	Density (g/cm³)	SSA (cm²/g)	Class
GBFS	39.91	12.9	2.33	32.04	6.44	0.85	0.75	0.4	0.23	3.83	2.8	5590	-
ÇAT	60.12	25.63	2.81	1.9	2.58	4.06	1.25	0.11	0.27	0.97	2.15	3370	F
KEM	34.65	15.27	3.93	35.4	1.8	1.49	0.67	5.58	0.32	0.53	2.71	2576	C
KAN	39.37	14.94	4.33	22.34	3.69	1.27	0.89	2.58	0.22	9.6	2.41	4124	C

*LOI: Loss on Ignition

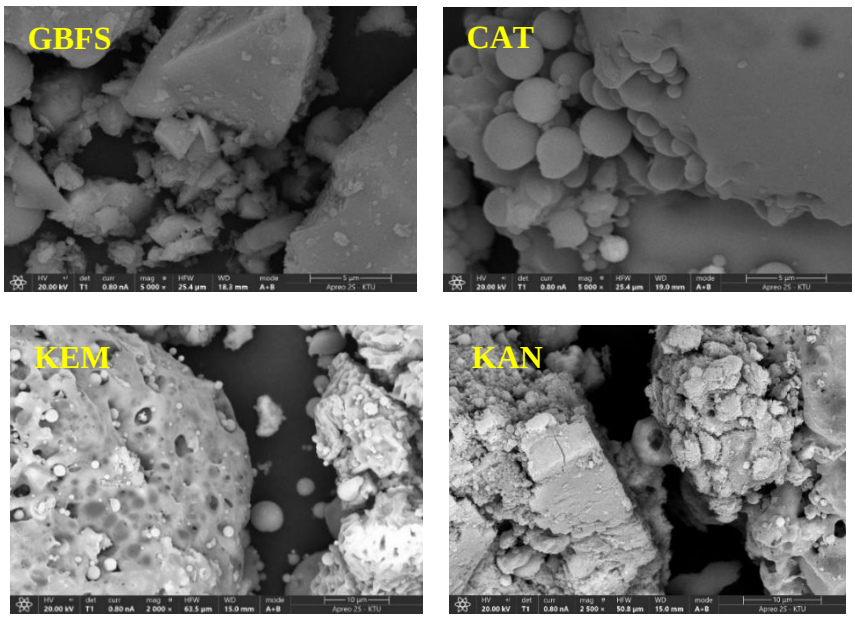


Figure 2. SEM images of binders used in GP production

Sodium hydroxide (NaOH) and powdered sodium metasilicate pentahydrate ($Na_2SiO_3{\cdot}5H_2O$) were used as alkaline activators. The sodium metasilicate pentahydrate had a SiO_2/Na_2O mass ratio of 1.0. NaOH has a molar mass of 39.99 g/mol and a density of 2.15 g/cm^3, while $Na_2SiO_3{\cdot}5H_2O$ has a molar mass of 212.14 g/mol and a density of 1.35 g/cm^3. The NaOH and $Na_2SiO_3{\cdot}5H_2O$ were dissolved separately in water. Once the prepared solutions cooled down to laboratory temperature, they were used together during the preparation of the mixtures.

Initial experimental designs targeted a constant water-to-binder (w/b) ratio across all GP mixtures [29,18,30]; however, distinct variations in precursor chemical compositions and physical properties necessitated dynamic w/b adjustments. A Vicat procedure, adapted from TS EN 196-3 [29], was therefore used as an operational consistency criterion for the activated pastes and the water-only reference pastes. Therefore, the optimum w/b ratio was determined separately for each binder and silicate modulus. For this purpose, standard consistency tests were performed using a Vicat apparatus in accordance with TS EN 196-3 [31]. These tests were conducted on both the activated mixtures (Ms ranging from 0.2 to 0.8) and the reference pastes consisting only of water and binder. The standard consistency criterion was defined as the amount of liquid required for the Vicat plunger to settle 5-7 mm from the bottom plate of the mold. The pastes were placed into the mold without any additional compaction or vibration. The appropriate w/b ratio for each binder and Ms value was determined based on the plunger penetration depth 30 seconds after release.

A coding system was used to name the GP mixtures, indicating both the type of precursor and the silicate modulus of the activator. In this coding system, the first part indicates the binder type, and the second part indicates the Ms value. For example, CAT/0.2 represents a mixture prepared with CAT fly ash at an Ms of 0.2, while GBFS/0.6 represents a mixture prepared with granulated blast furnace slag at an Ms of 0.6. A total of 16 GP mixtures were prepared using the four binders and four silicate modulus levels. The mixture proportion, Ms, alkaline activator parameters and w/b ratios are presented in Table 2.

Table 2. Compositions and activation parameters of GP mixtures

GP Pastas	NaOH (g)	$Na_2SiO_3{\cdot}5H_2O$ (g)	Ms	SiO_2/Binder (%)	Na_2O/Binder (%)	Na^+/Binder (%)	Water in the activator solution (g)	Water from $Na_2SiO_3{\cdot}5H_2O$ (g)	Total Water (g)	Total w/b
GBFS/0.0	0,0	0,0	0,0	0,0	0,0	0,0	1050,0	0,0	1050,0	0,350
CAT/0.0							660,0		660,0	0,220
KEM/0.0							1050,0		1050,0	0,350
KAN/0.0							2040,0		2040,0	0,680
GBFS/0.2	154,3	110,0	0,2	1,0	5,0	3,8	1005,0	46,7	1051,7	0,351
CAT/0.2							705,0		751,7	0,251
KEM/0.2							1065,0		1111,7	0,371
KAN/0.2							2015,0		2061,7	0,687
GBFS/0.4	115,0	215,0	0,4	2,0	5,0	3,8	985,0	91,3	1076,3	0,359
CAT/0.4							665,0		756,3	0,252
KEM/0.4							955,0		1046,3	0,349
KAN/0.4							1985,0		2076,3	0,692
GBFS/0.6	70,0	301,0	0,6	2,8	4,8	3,5	960,0	127,8	1087,8	0,363
CAT/0.6							635,0		762,8	0,254
KEM/0.6							930,0		1057,8	0,353
KAN/0.6							1950,0		2077,8	0,693
GBFS/0.8	26,3	342,4	0,8	3,2	4,0	3,0	960,0	145,4	1105,4	0,369
CAT/0.8							630,0		775,4	0,259
KEM/0.8							960,0		1105,4	0,369
KAN/0.8							1950,0		2095,4	0,699

** A constant binder mass of 3000 g was used for all four binder types.*

During specimen preparation, the alkaline activator solutions were first prepared and allowed to cool to ambient laboratory temperature. The geopolymer (GP) mixtures were then homogenized using a mixer for 3 min and cast into 40x40x160 mm prismatic molds with slight vibration. After casting, the molds containing the specimens were sealed in airtight, heat-resistant bags and cured in an oven at 60 °C for 24 h [32,33]. After heat curing, the samples were demolded and stored under ambient laboratory conditions until the testing days. Fresh and dry unit weight, flexural strength, compressive strength, and ultrasonic pulse velocity (UPV) tests were performed according to the TS EN 12390-7 [34], TS EN 12390-5 [35], TS EN 12390-3 [36], and ASTM C597-22 [37], respectively. The physical and mechanical properties were determined at the ages of 1, 7, and 28 days, while compressive and flexural strength measurements were also repeated on day 90. Three specimens were tested for each series, and the average values were reported.

3. Results and Discussion

3.1. Effect of Binder Characteristics on the Water-to-Binder Ratio

Differences in the chemical composition, fineness, and particle morphology of the binders significantly affected the water demand of the geopolymer pastes. The w/b ratios determined by the Vicat tests are presented in Figure 3, and the basic properties of the binders are

summarized in Table 3. Based on the test results, the lowest water demand was observed in the CAT-based mixtures, while the highest was recorded in the KAN-based mixtures.

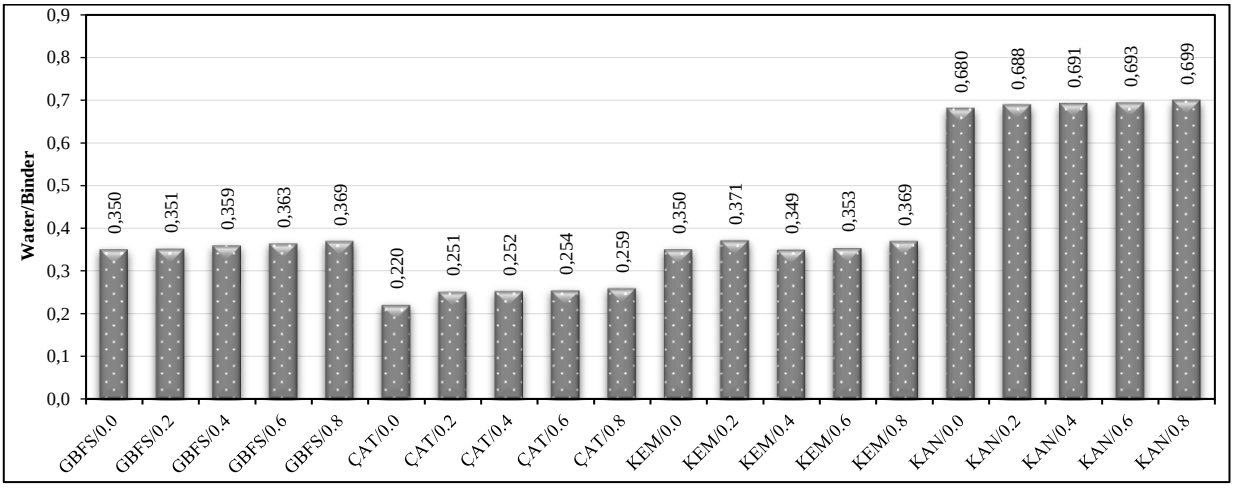


Figure 3. Water-to-binder (w/b) ratios determined by standard consistency tests for each binder type

Table 3. Basic properties of the binders and water-to-binder (w/b) ratios of the GP mixtures

Binder	Blaine specific surface area (cm²/g)	Loss on ignition (%)	CaO (%)	SEM morphology observation	w/b ratios
GBFS	5590 (Very fine)	3.83 (Moderate)	32.04 (High)	Angular and dense particles	0.35–0.37
CAT	3370 (Moderate)	0.97 (Very low)	1.90 (Very low)	Smooth-surface, distinct spherical structures	0.22–0.26
KEM	2576 (Coarse)	0.53 (Very low)	35.40 (Very high)	Large, porous, agglomerated, spherical and irregular structures	0.35–0.37
KAN	4124 (Fine)	9.60 (Very high)	22.34 (Moderate)	Irregular, fragmented forms and high surface porosity	0.68–0.70

GBFS has the highest Blaine specific surface area among the binders used in this study, at 5590 cm²/g. This high fineness can increase the water demand of the mixture because it increases the surface area of the particles in contact with the liquid phase [2]. In addition, the 32.04% CaO content of the GBFS and the angular particle morphology observed in the SEM images also influenced the fresh mixture behavior. Increased contact and friction between these angular particles can limit fluidity [38]. The high CaO content, which promotes the rapid formation of reaction products during alkali activation, is also considered another factor affecting the consistency of the pastes [5]. Under the combined effect of these properties, the w/b ratio for GBFS-based mixtures was determined to be in the range of 0.35–0.37.

CAT, the Class F fly ash, had lower water demand than the other fly ashes, with w/b ratios of 0.22–0.26. It contained 1.90% CaO and had an LOI of 0.97%. Lower water demand and better workability have also been reported for geopolymer mixtures containing low-calcium fly ash [39,40]. CAT's low LOI suggests that water adsorption by unburned carbon was limited [8]. Particle shape offers a further explanation: SEM images showed smooth, spherical particles, which can ease particle movement by reducing interparticle friction [41].

KEM required w/b ratios of 0.35–0.37, even though its Blaine specific surface area was the lowest (2576 cm²/g) and its LOI was only 0.53%. Neither fineness nor LOI alone explains why KEM required more water than CAT. Its CaO content of 35.40% may have contributed, given the increased water demand reported for some high-calcium fly ashes [42]. We also observed large, porous, irregular agglomerates in the SEM images. Water retained within these structures could reduce the free water available for flow [39]. Together, these observations point to contributions from both chemical composition and particle morphology, although the present results do not isolate their individual effects.

KAN-based systems are distinctly different from the other binders, with a w/b ratio of 0.68–0.70. KAN's high Blaine specific surface area (4124 cm^2/g) increases water demand by expanding the particle surface area interacting with the liquid phase [24]. However, the most prominent reason for the high-water demand in this series is the LOI value of 9.60%. A high LOI indicates a high amount of unburned carbon in the fly ash; water adsorption by these carbonaceous and porous particles can reduce the amount of available free water in the fresh mix [8,23]. The SEM images agree: KAN particles are irregular, fragmented, and porous [43]. This morphology, together with high fineness, high CaO content, and a high LOI, explains why KAN demands so much water.

Water demand tracks LOI and fineness across the binders (Figure 4). KAN reaches the highest w/b ratio, in line with its high LOI and relatively high Blaine surface area. CAT sits at the opposite end: its low LOI, low CaO content, and spherical particles allow it to achieve workability with the least water. In contrast, although GBFS and KEM have similar w/b ranges, their significant differences in fineness and LOI indicate that the water demand is not controlled by a single parameter. A predictive regression with LOI, CaO, and Blaine fineness would require four coefficients when an intercept is included, but the dataset contains only four independent precursor compositions. Such a model has zero residual degrees of freedom at precursor level and cannot provide a defensible error estimate or validated predictive equation. The four modulus formulations for each precursor do not create additional independent precursor chemistries. Figure 4 is therefore descriptive. More independently sampled ashes and slags, repeated consistency measurements, and external validation are needed before a transferable water-demand model can be developed.

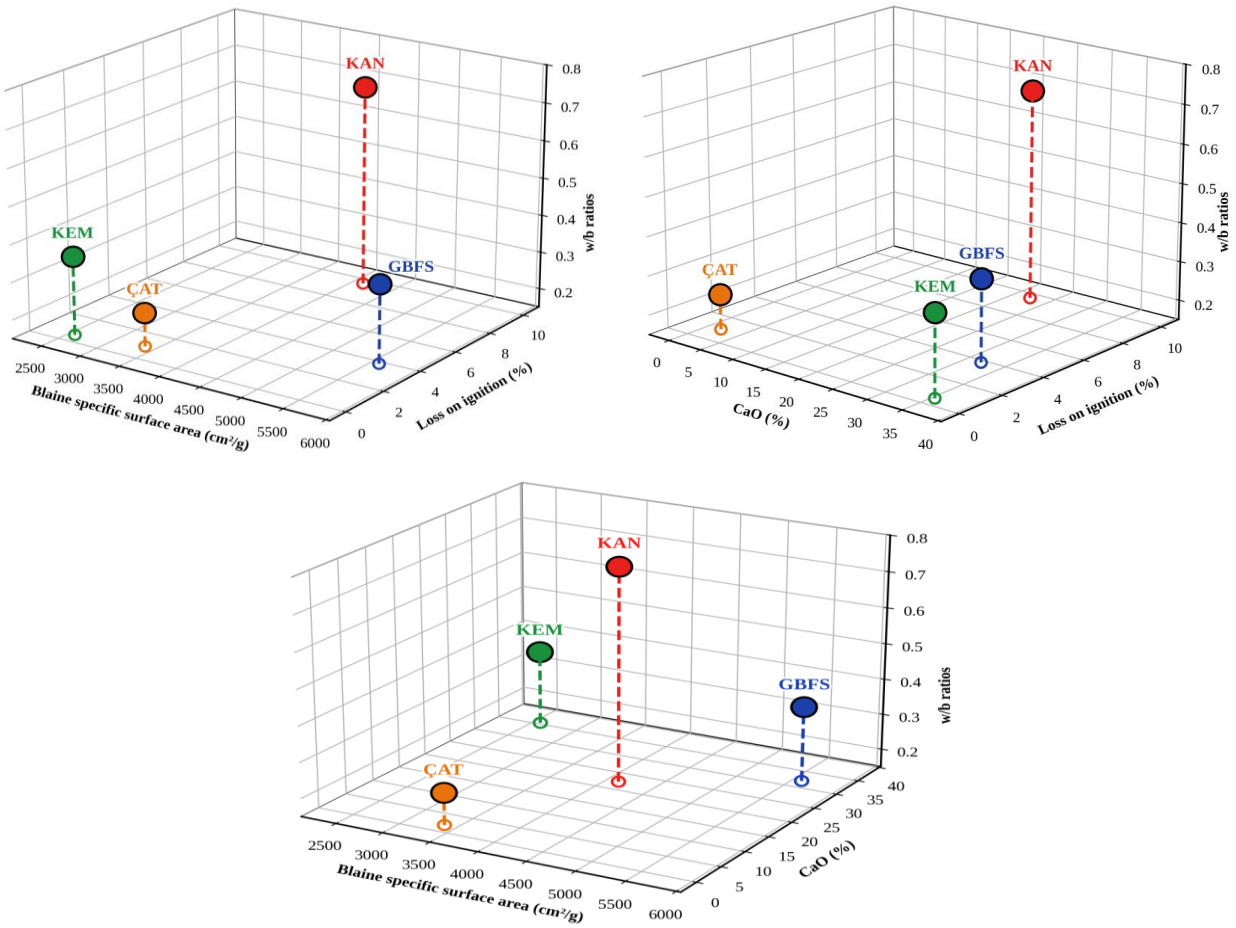


Figure 4. Relationship of Blaine specific surface area, loss on ignition (LOI), and CaO content with the water-to-binder (w/b) ratio

3.2. Physical Properties of Geopolymer Pastes

The fresh unit weight (FUW) and dry unit weight (DUW) values at different curing ages, as well as the average water-to-binder (w/b) ratios of the geopolymer pastes, are presented in Table 4. After heat curing, the specimens were demolded and stored under ambient laboratory conditions until the scheduled testing ages. The dry unit weight was determined on the day of measurement using the specimens stored under these conditions, without additional oven drying.

Differences in precursor density, water content, and volume change can all affect these measurements. In particular, the high initial water content of KAN dilutes the solids volume and increases the potential for capillary voids after water removal. Density measurements alone cannot distinguish water loss, solid loss, shrinkage, and changes in reaction products. The results indicate that the variation in unit weight is not solely dependent on the specific gravity of the binder; the amount of water in the mixture and the mass loss during curing are also determining factors. In particular, in systems with high w/b ratios, the higher water content in the fresh mixture reduced the FUW values. In contrast, moisture loss from the system during curing further decreased the DUW values.

Table 4. FUW, DUW, and w/b ratios of the GP pastes

Binder	Specific gravity of the binder (g/cm³)	FUW (g/cm³)	Curing age-dependent dry density (g/cm³)				w/b ratios
			1-day	7-days	28-days	D.O. *	
GBFS	2.80	1.97	1.96	1.95	1.95	0.56%	0.36
CAT	2.15	1.67	1.67	1.63	1.58	5.39%	0.25
KEM	2.71	1.82	1.80	1.79	1.79	0.55%	0.36
KAN	2.41	1.48	1.42	1.37	1.30	8.45%	0.69

* D.O. denotes the reported percentage decrease in DUW from day 1 to day 28. Densities are rounded to two decimal places; small differences between percentages and calculations from the displayed values require checking against the unrounded measurements. D.O. is not measured porosity.

KAN pastes had the lowest FUW of all series (1.48 g/cm³), although the binder particle density was 2.41 g/cm³. Their high average w/b ratio of 0.69 helps explains this difference. DUW decreased during curing to 1.42, 1.37, and finally 1.30 g/cm³, with an 8.45% reduction between days 1 and 28. This decrease is consistent with the loss of water that had not become bound within the reaction products, although unit weight measurements alone cannot establish the amount of unbound water. The surface bleeding and efflorescence we observed provide further evidence of water movement and the transport of dissolved alkali.

Although CAT had the lowest binder particle density (2.15 g/cm³), its pastes had higher fresh and dry unit weights than KAN. At an average w/b ratio of 0.25, CAT pastes had an FUW of 1.67 g/cm³ and a 28-day DUW of 1.58 g/cm³. This difference is consistent with CAT's lower water demand: the unit weights of the two paste systems did not match the relative densities of their precursors.

In the GBFS and KEM-based pastes, the difference between FUW and DUW remained quite limited. In the GBFS series, the FUW value, which was 1.97 g/cm³, decreased to 1.95 g/cm³ on day 28, while in the KEM series, the FUW value, which was 1.82 g/cm³, decreased to 1.79 g/cm³. The change between days 1 and 28 in both series is approximately 0.55%. The similar w/b ratios and minimal mass loss during curing observed in GBFS and KEM indicate the development of a highly stable physical matrix. However, the higher binder density of GBFS contributed to it showing a higher unit weight than KEM under the same water conditions.

The effects of silicate modulus on FUW and DUW are given in Figure 5. In GBFS-based pastes, as the Ms value increased to 0.6 and 0.8, FUW reached approximately 1.98 g/cm³, while there was only a limited change in DUW values at 1, 7, and 28 days. This indicates that no significant mass loss occurred during the curing process and that the GBFS-based matrix largely maintained its physical integrity. A similar trend was observed in KEM-based pastes; the low difference between FUW and DUW suggests that this system also has a relatively stable structure.

In CAT-based systems, a more pronounced change was observed depending on the silicate modulus. The highest FUW value was determined as 1.70 g/cm³ at Ms = 0.2, while the DUW value decreased to 1.53 g/cm³ on day 28 when the Ms was increased to 0.8. This trend suggests that mass loss increases during curing at high silicate moduli, and the way water is retained within the matrix changes. However, it is not possible to directly attribute this behavior to a specific gel formation mechanism based solely on FUW and DUW data; therefore, density change was considered as an indicator of physical stability.

The fact that the difference between FUW and DUW in the KAN series is higher than in the other binders is consistent with the high-water requirement determined in the previous section. The high w/b ratio led to the presence of more free water in the fresh mixture; the removal of this water during curing significantly reduced the DUW values. The bleeding observed in the samples also supports this interpretation. When a sufficiently consistent and stable reaction matrix is not developed, the inability to retain excess water in the mixture can increase both mass loss and physical instability [8]. In general, while a low FUW–DUW difference in GBFS and KEM-based pastes indicates more limited mass loss, the high w/b ratio, bleeding, and high DUW loss in the KAN series revealed weaker physical stability.

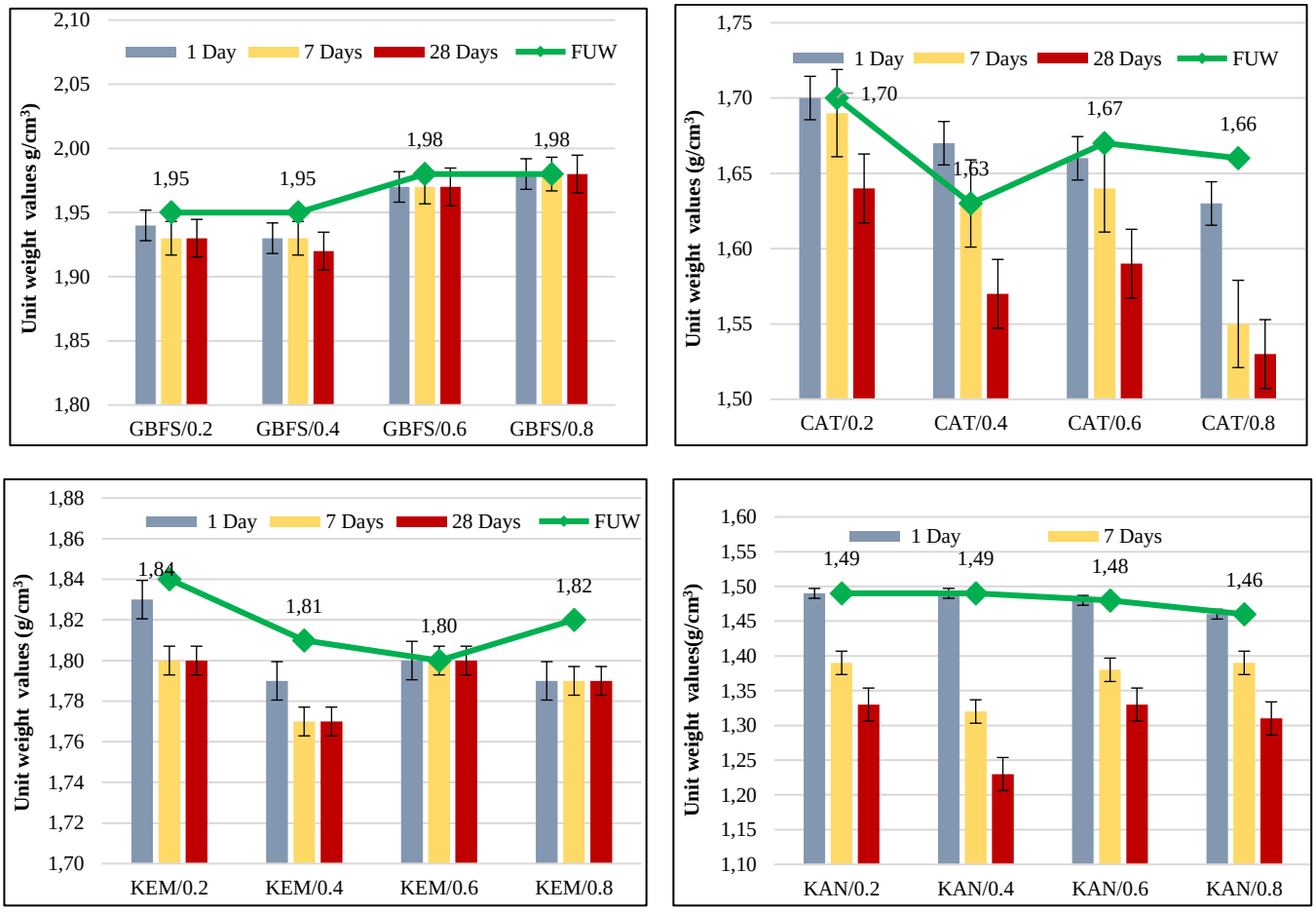


Figure 5. FUW and DUW values of the GP pastes depending on the silicate modulus

3.3. Effect of Binder Type and Silicate Modulus on Mechanical Properties

The 1-, 7-, 28-, and 90-day compressive strengths of the geopolymer pastes are presented in Figure 6. The results indicate that strength development varied significantly depending on both the binder type and the silicate modulus. The chemical composition, specific surface area, and particle properties of the binders are among the key parameters affecting the alkali activation process and the associated mechanical performance [16]. The fact that the investigated binders did not show similar strength trends at the same Ms value reveals that the optimum activation conditions depend on the properties of the precursor material.

GBFS-based pastes exhibited the highest compressive strength among the investigated binders. The combination of a Blaine specific surface area of 5590 cm²/g and a CaO content of 32.04% is the main feature contributing to its high reactivity in an alkaline environment. The compressive strength increased up to an Ms = 0.6, reaching the highest value in the study (82.25 MPa) at this modulus level. Increasing the Ms value to 0.8 did not provide an additional increase in strength. It has been reported that high silicate content can increase the viscosity of the activator solution, limiting ion mobility and the dissolution of the precursor [44]. Therefore, the results obtained by GBFS show that Ms = 0.6 provides a more suitable activation environment under the studied conditions.

CAT pastes gained compressive strength as Ms increased to 0.6, but strength fell at Ms = 0.8. Their low water demand, discussed in the previous section, and smooth, spherical particles likely favored matrix development. CAT also had low CaO (1.90%) and LOI (0.97%) contents, although the strength results do not establish the contribution of each characteristic. The response to Ms agrees with reports that soluble silicate can support reaction in low-calcium fly ash systems up to a certain concentration, beyond which it can hinder dissolution and subsequent reactions [30].

KEM pastes reached their highest compressive strength at Ms = 0.4; strength decreased as Ms increased further. Although KEM contained more CaO (35.40%) than the other precursors, its low Blaine specific surface area (2576 cm²/g) and the large, porous particles and agglomerates visible in the SEM images suggest that particle characteristics limited the potential benefit of its calcium content. The decline above Ms = 0.4 could reflect a further constraint on reaction: excess soluble silicate can hinder precursor dissolution and subsequent reactions in some alkali-activated systems [20]. This mechanism remains a possible explanation for the KEM results rather than a directly verified finding.

KAN-based pastes, on the other hand, showed lower and less stable strength development compared to the other three binders. Although KAN's Blaine specific surface area of 4124 cm²/g and 22.34% CaO content offer certain reaction potential, its LOI value of 9.60%, the increase in the water-to-binder ratio to 0.69, and irregular, porous particle structure stand out as the main features limiting the mechanical performance of the system [8]. The high-water demand and bleeding observed in the previous sections also indicated that the physical stability of this series is lower than that of the other binders. The inability to determine the 90 day compressive strength for KAN/0.8 pastes is attributed to excess activator which does not participate in the alkali activation process leaking out through the capillary pores and causing the structure to deteriorate.

When the binders were evaluated together, the highest compressive strength performance was obtained in GBFS-based pastes, followed generally by the CAT and KEM series. KAN, on the other hand, showed the lowest mechanical performance among all series. However, a more important finding is that the Ms value at which the highest strength is obtained varies depending on the binder. While the optimum value for GBFS and CAT is around Ms = 0.6, the highest performance for KEM was obtained at Ms = 0.4. In KAN-based mixtures, increasing the silicate modulus did not eliminate the negative aspects associated with its high-water demand and physical instability.

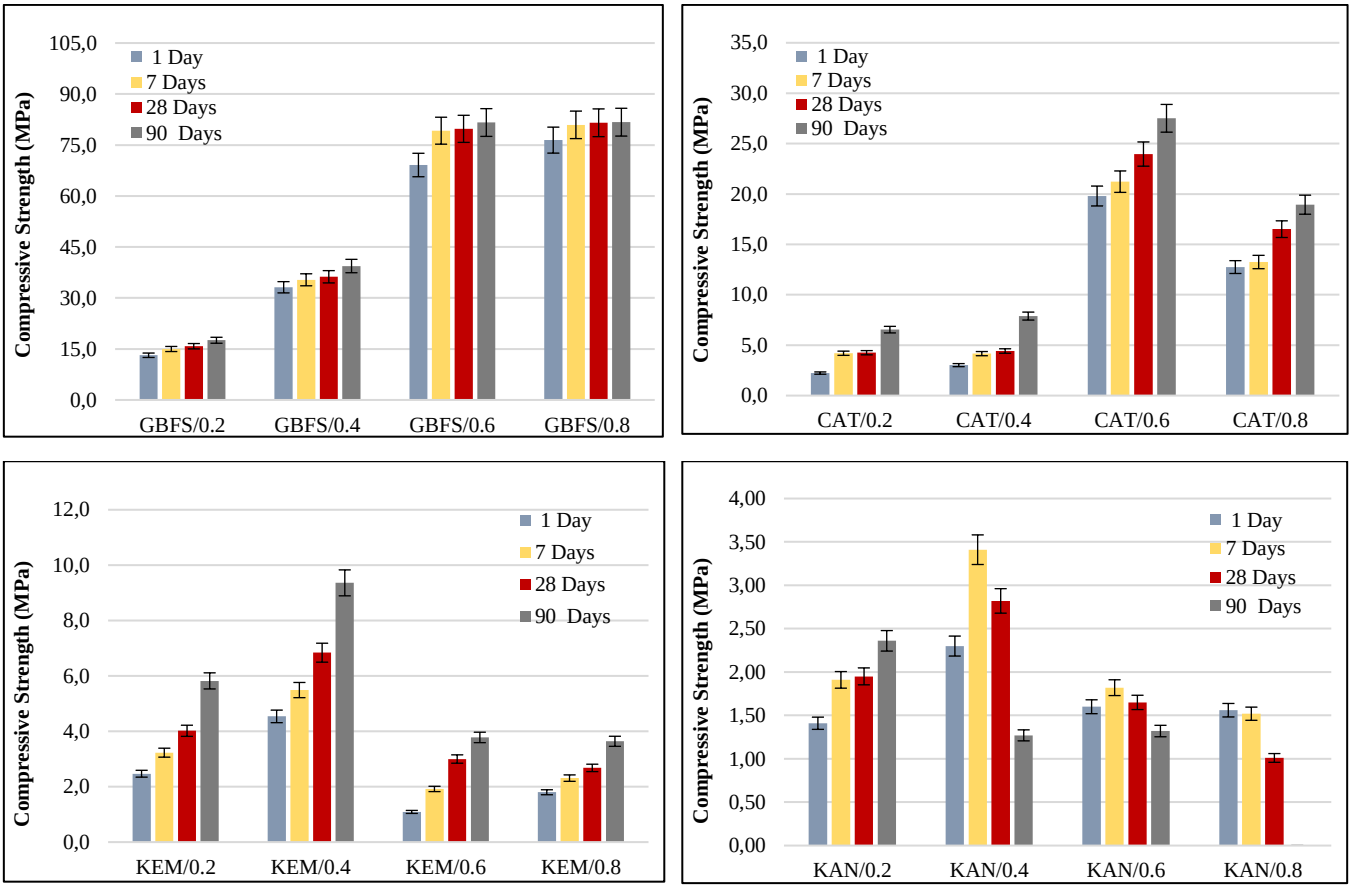


Figure 6. Compressive strengths of the GP pastes depending on the silicate modulus and curing age

The 1-day, 7-days, 28-days, and 90-days flexural strengths of the geopolymer pastes are presented in Figure 7. In general, the flexural strength results are consistent with the trends observed in the compressive strength tests. In the GBFS-based pastes, the flexural strength increased up to an Ms = 0.6, reaching its highest value of 4.91 MPa at this modulus level. The higher performance achieved in both flexural and compressive strengths can be attributed to the high fineness of GBFS and the contribution of its CaO content to the development of alkali activation products.

In the CAT-based pastes, the highest flexural strength was again obtained at Ms = 0.6, while the strength decreased at higher silicate modulus. This trend is consistent with the compressive strength results and aligns with literature findings indicating that a silicate content above a certain threshold may limit the reaction process in low-calcium fly ash systems [20,18]. In the KEM series, the increase in flexural strength up to an Ms = 0.4 and its subsequent decrease at higher modulus also parallel the optimum Ms value determined for compressive strength. It is believed that the low specific surface area and large, agglomerated particle structure of KEM, despite its high CaO content, limit the development of a more homogeneous matrix. In the KAN-based pastes, the lowest flexural strengths were obtained, which is consistent with its high LOI, high water demand, and physical instability [45].

In conclusion, the flexural strength data demonstrate that the mechanical performance ranking of the binder types is largely similar to that of the compressive strength. Furthermore, the similarity of the optimum Ms values in both mechanical properties for a given binder supports the decisive role of the relationship between the silicate modulus and the precursor material properties on mechanical performance.

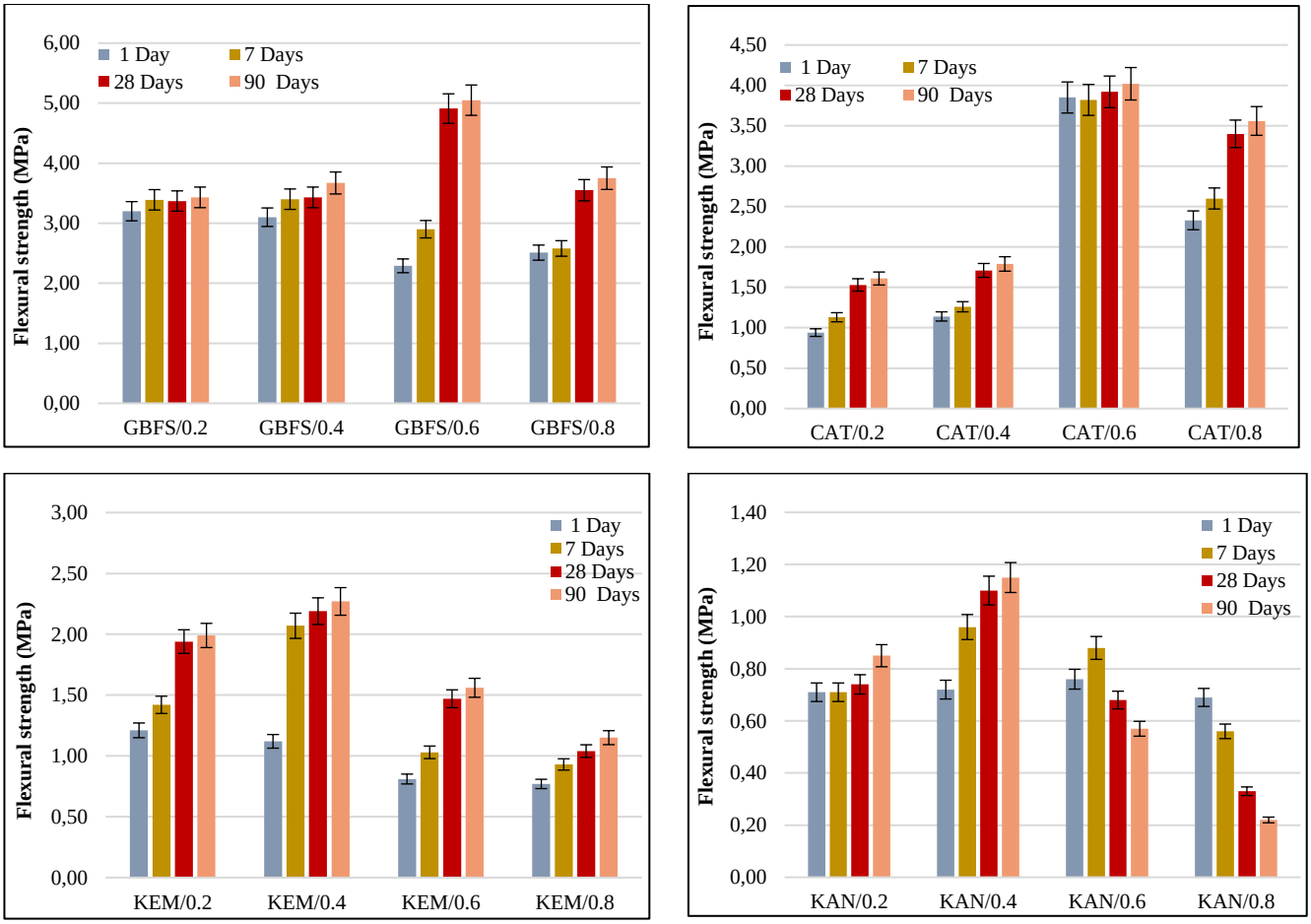


Figure 7. Flexural strengths of the GP pastes depending on the silicate modulus and curing age

Figure 8 illustrates the development of ultrasonic pulse velocity (UPV) in the geopolymer pastes over 1, 7, and 28 days of curing. The UPV values varied depending on the binder type and silicate modulus and generally exhibited a trend similar to the mechanical strength results. The highest UPV values were obtained in the GBFS series; at Ms = 0.6 and 0.8, the 28-day UPV values reached 3.65 km/s. This result indicates that GBFS pastes develop a more continuous and dense internal structure compared to the other binders [29,6].

In the CAT series, the highest UPV value was measured as 2.40 km/s at Ms = 0.6, while a limited decrease occurred at Ms = 0.8 [18]. In the KEM series, the highest value was determined as 2.20 km/s at Ms = 0.4, and the UPV decreased at higher silicate modulus. The fact that the optimum Ms values determined for UPV in both binders coincide with the values determined for compressive and flexural strengths supports the strong relationship between mechanical performance and matrix integrity.

The KAN series exhibited consistently low UPV values, ultimately failing to yield measurable data at 28 days for the Ms = 0.8 mixtures due to structural degradation. This is consistent with the high-water demand, mass loss, and mechanical strength loss observed in this series [8]. The similar trends in the UPV, compressive, and flexural strength results generally indicate that the variation in the mechanical performance of geopolymer pastes is closely related to the physical integrity and densification of the matrix.

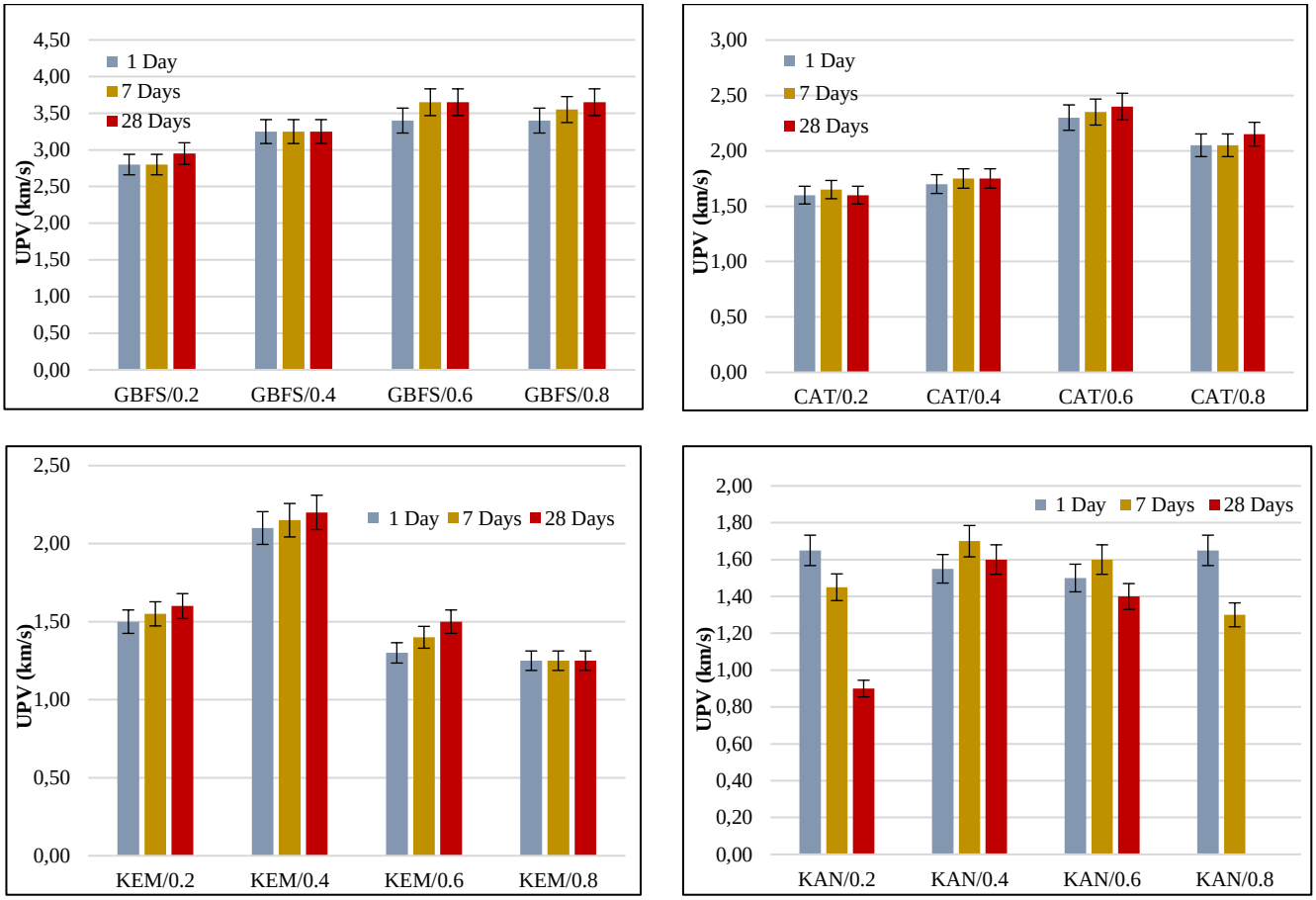


Figure 8. Ultrasonic pulse velocity (UPV) values of the GP pastes depending on the silicate modulus and curing age

4. Conclusion

The study compares 16 consistency-adjusted alkali-activated paste formulations derived from four industrial by-products, each with a nominal Ms value between 0.2 and 0.8. The conclusions apply to the tested water contents and varying alkali dosages, as well as a common heat-curing schedule of 60 °C.

- Vicat-based water demand ranged from w/b = 0.251–0.259 for CAT to 0.688–0.699 for KAN. The contrast is associated with differences in LOI, calcium content, fineness, and morphology. Four precursor compositions are insufficient to quantify the independent effect of each property or validate a multivariable prediction equation.
- GBFS reached reported peak compressive and flexural strengths of 82.25 and 4.91 MPa at nominal Ms = 0.6. This was the best-performing GBFS formulation tested; neither a continuous nor a statistically established optimum was determined.
- CAT and KEM showed their highest measured mechanical performance at nominal Ms = 0.6 and 0.4, respectively. Higher bulk CaO alone did not ensure higher strength. These formulation-specific maxima include the effects of changing Na_2O dosage and water content.
- KAN combined high water demand with bleeding, declining density, and low mechanical performance. Its 8.45% reported density reduction between days 1 and 28 is not a measured porosity. High initial water content and segregation are plausible major physical limitations, but their contributions cannot be separated from chemical effects. The unavailable 28-day UPV result and reported 90-day loss of integrity of KAN/0.8 do not establish a specific expansive reaction.
- UPV generally followed the same mechanical trends as the other pastes, reaching a maximum value of 3.65 km/s in GBFS. While these values enable relative comparisons between the tested pastes, they do not establish concrete quality classes or provide calibrated strength predictions. Distinguishing between chemical reactivity, physical dilution, and damage requires quantitative phase analysis, direct porosity measurements, and comparisons of controlled water.

Future work should investigate the impact of mechanical or thermal pretreatment on GBFS–KAN blends, using a controlled total dosage of water and Na_2O. While blending can reduce the proportion of high-LOI ash and introduce a more reactive calcium-bearing component, this must be demonstrated through experimentation [8, 24, 25]. Such studies should combine quantitative XRD analysis, imaging of the hardened paste, bleeding and shrinkage measurements, and mechanical test replication. Durability and environmental assessments are also required before these formulations can be recommended for use in construction projects.

Author Contributions

H.E.: Formal Analysis, Investigation,
M.Ç.: Conceptualization, Methodology, Writing – Original Draft,
İ.D.: Writing – Original Draft, Writing – Review & Editing

Funding

The authors would like to thank the Kırıkkale University Scientific Research Projects Funding Office for its financial support of this study (Project Nos: 2024/128).

Data Availability Statement

The data presented in this study are available from the corresponding author upon reasonable request.

Conflict of Interest Statement

The authors declare that there is no conflict of interest. They have no known competing financial interests or personal relationships that could have appeared to influence the work reported in this paper.

Acknowledgment

This study was conducted as part of the Ph.D. thesis work of Hüseyin ERSOY.

References

[1.] Criado, M., Palomo, A., Fernandez-Jimenez, A., Alkali activation of fly ashes Part 1: Effect of curing conditions on the carbonation of the reaction products. Fuel 84(16) (2005) 2048–2054.

[2.] Saedi, M., Behfarnia, K., Soltanian, H., The effect of the Blaine fineness on the mechanical properties of the alkali-activated slag cement. Journal of Building Engineering 26 (2019) 100897.

[3.] Öz, H.Ö., Doğan-Sağlamtimur, N., Bilgil, A., Tamer, A., Günaydın, K., Process development of fly ash-based geopolymer mortars in view of the mechanical characteristics. Materials 14(11) (2021) 2935.

[4.] Anand, S., Vrat, P., Dahiya, R.P., Application of a system dynamics approach for assessment and mitigation of CO2 emissions from the cement industry. Journal of Environmental Management 79(4) (2006) 383–398.

[5.] Chindaprasirt, P., Chareerat, T., Sirivivatnanon, V., Workability and strength of coarse high calcium fly ash geopolymer. Cement and Concrete Composites 29(3) (2007) 224–229.

[6.] Ye, W., Kruppa, H., Vollpracht, A., Tan, Y., Rheological behavior of siliceous fly ash geopolymer paste and mortar workability. Construction and Building Materials (2025) 142050.

[7.] Bai, T., Song, Z.G., Wang, H., Wu, Y.G., Huang, W., Performance evaluation of metakaolin geopolymer modified by different solid wastes. Journal of Cleaner Production 226 (2019) 114–121.

[8.] Manzi, S., Saccani, A., Baldazzi, L., Lancellotti, I., Mix-design and properties of mortars from alkali-activated fly ashes containing high amounts of unburned carbon matter. International Journal of Concrete Structures and Materials 14 (2020) 59.

[9.] Zhang, Z.H., Zhu, H.J., Zhou, C.H., Wang, H., Geopolymer from kaolin in China: An overview. Applied Clay Science 119 (2016) 31–41.

[10.] Davidovits, J., Geopolymers: Ceramic-like inorganic polymers. Journal of Ceramic Science and Technology 8(3) (2017) 335–350.

[11.] Davidovits, J., Geopolymers: Inorganic polymeric new materials. Journal of Thermal Analysis and Calorimetry 37(8) (1991) 1633–1656.

[12.] Qaidi, S.M., Tayeh, B.A., Zeyad, A.M., de Azevedo, A.R., Ahmed, H.U., Emad, W., Recycling of mine tailings for the geopolymers production: A systematic review. Case Studies in Construction Materials 16 (2022) e00933.

[13.] Öksüzer, N., Atık çay külünün çimentosuz geopolimer karışımlarda silika kaynağı olarak değerlendirilmesi. Black Sea Journal of Engineering and Science 8(6) (2025) 1998–2005.

[14.] Ward, C.R., French, D.H., Determination of glass content and estimation of glass composition in fly ash using quantitative X-ray diffractometry. Fuel 85(16) (2006) 2268–2277.

[15.] Puertas, F., Varga, C., Alonso, M.M., Rheology of alkali-activated slag pastes. Effect of the nature and concentration of the activating solution. Cement and Concrete Composites 53 (2014) 279–288.

[16.] Davidovits, J., Geopolymer Chemistry and Applications. Institut Géopolymère, Saint-Quentin, France, 2008.

[17.] Sevim, O., Demir, I., Alakara, E.H., Bayer, İ.R., Experimental evaluation of new geopolymer composite with inclusion of slag and construction waste firebrick at elevated temperatures. Polymers 15(9) (2023) 2127.

[18.] Adewumi, A.A., Mohd Ariffin, M.A., Maslehuddin, M., Yusuf, M.O., Ismail, M., Al-Sodani, K.A.A., Influence of silica modulus and curing temperature on the strength of alkali-activated volcanic ash and limestone powder mortar. Materials 14(18) (2021) 5204.

[19.] Kong, D.L.Y., Sanjayan, J.G., Sagoe-Crentsil, K., Comparative performance of geopolymers made with metakaolin and fly ash after exposure to elevated temperatures. Cement and Concrete Research 37(12) (2007) 1583–1589.

[20.] Firdous, R., Stephan, D., Effect of silica modulus on the geopolymerization activity of natural pozzolans. Construction and Building Materials 219 (2019) 31–43.

[21.] Hakeem, I.Y., Zaid, U., Arbili, M.M., Alyami, M., Alhamami, A., Alharthai, M., Ultra-high-performance geopolymer concrete: A state-of-the-art review of physical, durability, and microstructural characteristics. Heliyon 10(2) (2024) e24263.

[22.] ASTM D7348, Standard Test Methods for Loss on Ignition (LOI) of Solid Combustion Residues. ASTM International, 2021.

[23.] Atiş, C.D., Strength properties of high-volume fly ash roller compacted and workable concrete, and influence of curing condition. Cement and Concrete Research 35(6) (2005) 1112–1121.

[24.] Soutsos, M., Boyle, A.P., Vinai, R., Hadjierakleous, A., Barnett, S.J., Factors influencing the compressive strength of fly ash based geopolymers. Construction and Building Materials 110 (2016) 355–368.

[25.] Biricik, H., Sanrı Karapınar, I., Effect of slag fineness and curing conditions on the mechanical properties of alkali-activated blast furnace slag mortars. International Journal of Engineering Technologies 7(2) (2021) 33–38.

[26.] Marjanović, N., Komljenović, M., Baščarević, Z., Nikolić, V., Petrović, R., Physical-mechanical and microstructural properties of alkali-activated fly ash–blast furnace slag blends. Ceramics International 41(1B) (2015) 1421–1435.

[27.] Rafeet, A., Vinai, R., Soutsos, M., Sha, W., Effects of slag substitution on physical and mechanical properties of fly ash-based alkali activated binders (AABs). Cement and Concrete Research 122 (2019) 118–135.

[28.] ASTM C618-25a, Standard Specification for Coal Fly Ash and Raw or Calcined Natural Pozzolan for Use in Concrete. ASTM International, 2025.

[29.] Yadollahi, M.M., Benli, A., Demirboğa, R., The effects of silica modulus and aging on compressive strength of pumice-based geopolymer composites. Construction and Building Materials 94 (2015) 767–774.

[30.] Sivasakthi, M., Jeyalakshmi, R., Rajamane, N.P., Effect of change in the silica modulus of sodium silicate solution on the microstructure of fly ash geopolymers. Journal of Building Engineering 44 (2021) 102939.

[31.] TS EN 196-3, Çimento Deney Metotları – Bölüm 3: Priz Süresi ve Genleşme Tayini. Türk Standardları Enstitüsü, Ankara, Türkiye, 2016.

[32.] Bakharev, T., Thermal behaviour of geopolymers prepared using class F fly ash and elevated temperature curing. Cement and Concrete Research 36(6) (2006) 1134–1147.

[33.] Sajan, P., Jiang, T., Lau, C.K., Tan, G., Ng, K., Combined effect of curing temperature, curing period and alkaline concentration on the mechanical properties of fly ash-based geopolymer. Cleaner Materials 1 (2021) 100002.

[34.] TS EN 12390-7, Beton – Sertleşmiş Beton Deneyleri – Bölüm 7: Sertleşmiş Betonun Yoğunluğunun Tayini. Türk Standardları Enstitüsü, Ankara, Türkiye, 2019.

[35.] TS EN 12390-5, Beton – Sertleşmiş Beton Deneyleri – Bölüm 5: Deney Numunelerinin Eğilme Dayanımının Tayini. Türk Standardları Enstitüsü, Ankara, Türkiye, 2019.

[36.] TS EN 12390-3, Beton – Sertleşmiş Beton Deneyleri – Bölüm 3: Deney Numunelerinde Basınç Dayanımının Tayini. Türk Standardları Enstitüsü, Ankara, Türkiye, 2019.

[37.] ASTM C597-22, Standard Test Method for Ultrasonic Pulse Velocity Through Concrete. ASTM International, West Conshohocken, PA, USA, 2022.

[38.] Mohamed, O.A., Ghanam, O., Hamdan, A., Zuaiter, M., Kim, T.Y., Mechanical properties and durability of concrete with recycled air-cooled blast furnace slag aggregates. Scientific Reports 15 (2025) 24384.

[39.] Li, X., Jin, S., Yan, T., Qiao, X., Yuan, J., Unraveling the interactive effects of Na2O/Al2O3, SiO2/Al2O3 and calcium on the properties of geopolymers from circulating fluidized bed fly ashes. Case Studies in Construction Materials 21 (2024) e03798.

[40.] Samson, G., Cyr, M., Gao, X.X., Formulation and characterization of blended alkali-activated materials based on flash-calcined metakaolin, fly ash and GGBS. Construction and Building Materials 144 (2017) 50–64.

[41.] Du, S., Zhao, Q., Shi, X., High-volume fly ash-based cementitious composites as sustainable materials: An overview of recent advances. Advances in Materials Science and Engineering 2021 (2021) 4976169.
[42.] Kesikidou, F., Konopisi, S., Anastasiou, E.K., Influence of concrete sludge addition in the properties of alkali-activated and non-alkali-activated fly ash-based mortars. Advances in Civil Engineering 2021 (2021) 5534002.

[43.] Sagawa, Y., Ota, S., Harada, K., Nishizaki, T., Goda, H., Utilization of fly ash with higher loss on ignition for geopolymer mortar. Advanced Materials Research 1129 (2015) 614–620.

[44.] Cho, Y.K., Yoo, S.W., Jung, S.H., Lee, K.M., Kwon, S.J., Effect of Na2O content, SiO2/Na2O molar ratio, and curing conditions on the compressive strength of FA-based geopolymer. Construction and Building Materials 145 (2017) 253–260.

[45.] Sarıdemir, M., Çelikten, S., Effects of Ms modulus, Na concentration and fly ash content on properties of vapour-cured geopolymer mortars exposed to high temperatures. Construction and Building Materials 363 (2023) 129868.

How to Cite This Article

Ersoy, H., Çavuş, M., and Demir, İ., Precursor-Dependent Performance of Low-Silicate-Modulus Industrial Byproduct-Based Geopolymers, Civil Engineering Beyond Limits, 1 (2027), 11179.
https://doi.org/10.36937/cebel.2027.11179